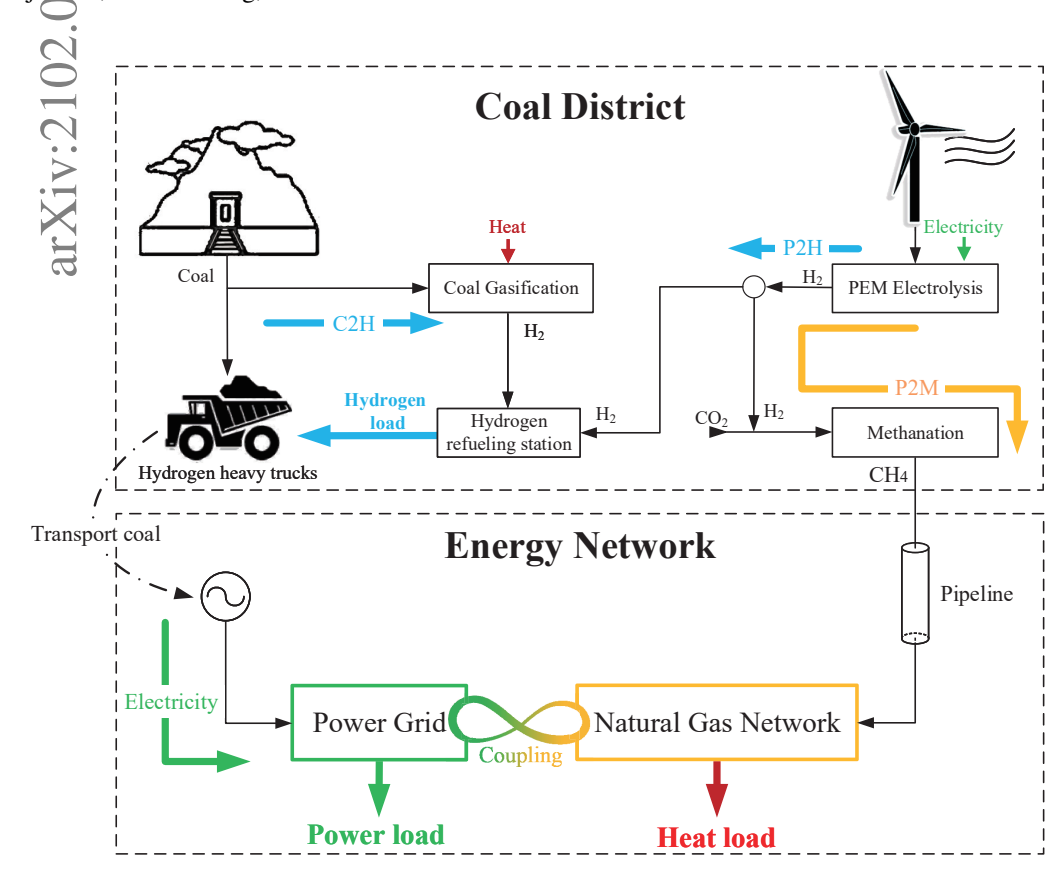
#### **Graphical Abstract**

Electricity-gas integrated energy system optimal operation in typical scenario of coal district considering hydrogen heavy trucks

Junjie in, Jianhua Wang, Jun You



#### Highlights

# Electricity-gas integrated energy system optimal operation in typical scenario of coal district considering hydrogen heavy trucks

Junjie Yin, Jianhua Wang, Jun You

- Advantages of hydrogen heavy trucks in typical scenario of coal industry district are discussed.
- The efficient closed loop of hydrogen energy from generation to utilization is proposed.
- P2G including power-to-hydrogen and power-to-methane is developed, combined with coal gasification technology.
- The economy and low-carbon properties of the proposed IEGS mechanism are analyzed.

# Electricity-gas integrated energy system optimal operation in typical scenario of coal district considering hydrogen heavy trucks

Junjie Yin<sup>a</sup>, Jianhua Wang<sup>a,\*</sup> and Jun You<sup>a</sup>

<sup>a</sup>School of Electrical Engineering, Southeast University, Nanjing 210096, China

#### ARTICLE INFO

# Keywords: Integrated energy system Power-to-gas Coal-to-hydrogen Hydrogen heavy trucks Second-order cone programming Optimized scheduling

#### ABSTRACT

The coal industry contributes significantly to the social economy, but the emission of greenhouse gases puts huge pressure on the environment in the process of mining, transportation, and power generation. In the integrated energy system (IES), the current research about the power-to-gas (P2G) technology mainly focuses on the injection of hydrogen generated from renewable energy electrolyzed water into natural gas pipelines, which may cause hydrogen embrittlement of the pipeline and cannot be repaired. In this paper, sufficient hydrogen energy can be produced through P2G technology and coal-to-hydrogen (C2H) of coal gasification, considering the scenario of coal district is rich in coal and renewable energy. In order to transport the mined coal to the destination, hydrogen heavy trucks have a broad space for development, which can absorb hydrogen energy in time and avoid potentially dangerous hydrogen injection into pipelines and relatively expensive hydrogen storage. An optimized scheduling model of electric-gas IES is proposed based on second-order cone programming (SOCP). In the model proposed above, the closed industrial loop (including coal mining, hydrogen production, truck transportation of coal, and integrated energy systems) has been innovatively studied, to consume renewable energy and coordinate multi-energy. Finally, an electric-gas IES study case constructed by IEEE 30-node power system and Belgium 24-node natural gas network was used to analyze and verify the economy, low carbon, and effectiveness of the proposed mechanism.

#### 1. Introduction

#### 1.1. Motivations

As we all know, the coal district is a typical large energy load of industry. In the production process of mining, preparation, etc., coal mine machineries need to consume a lot of electricity and heat. In addition, heavy trucks transport coal to various destinations, which requires a large amount of energy to drive the engine and is essential in the coal industrial production process. Moreover, the coal industry areas usually suffer from serious environmental pollution problems, the main reasons include but not limited to coal dust, factory emissions, vehicle exhaust, etc. Facing the tremendous environmental pressure and resource shortage, coal districts that rely on traditional energy supply methods are in urgent need of transformation.

Nowadays, the development of renewable energy, represented by wind power (WP), solar photovoltaics (PV), etc., has become an inevitable trend. Generally speaking, coal resources are distributed in inland mountainous areas, and the local geographical features determine the abundant WP resources in these areas. However, the phenomenon of abandoning WP and PV is still serious, mainly due to the instability of renewable energy and the difficulty of being directly integrated into traditional energy networks.

Based on the above analysis, an energy mechanism for the typical coal districts has yet to be proposed. For coal districts, there are the following visions: giving full play to the advantages of rich wind energy in coal districts, design-

wangjianhua@seu.edu.cn (J. Wang)

ORCID(s): 0000-0001-7782-7274 (J. Yin); 0000-0001-5185-4506 (J.

and realizing smooth, low-carbon and environment-friendly transportation of coal resources. As an energy output terminal, it has important responsibilities for the entire energy network. Therefore, the following goals should be achieved: consuming renewable energy as much as possible, breaking the status quo of the separate design and independent operation of each existing energy supply system, and establishing the integrated energy system (IES), in order to promote the optimization of the energy structure and finally achieve the grand goal of carbon neutrality.

ing practical and effective energy supply structure systems,

#### 1.2. Related Work

Regarding IES, many studies mainly focuse on the coupling and interaction of power systems and natural gas systems, i.e., integrated electric-gas systems (IEGS) [1, 2]. According to the type of conversion gas, Power-to-gas (P2G) technology can be divided into two types: power-to-hydrogen (P2H) conversion and power-to-methane (P2M) conversion. The hydrogen and methane produced in P2G plants can be used in following ways [3]:

- (1) Further synthesis to methane or other hydrocarbon fuels through methanation equipment;
- (2) Injection the mixture of hydrogen and methane into natural gas pipelines by hydrogen compressed natural gas (HCNG) technology [4];
- (3) Power generation with the help of internal combustion engine or combined heat and power (CHP) devices [5];
- (4) Hydrogen storage into tanks after pressurization [6];
- (5) Hydrogen refueling stations for vehicles or the use of hydrogen in industry.

<sup>\*</sup>Corresponding author

#### **Nomenclature**

Abbreviations		$\alpha_{{ m H}_2,t}$	Power consumption parameter corresponding to H <sub>2</sub>
C2H	Coal-to-hydrogen of coal gasification	$\beta_t$	Ratio of mined coal used as the raw material for coal
<b>IEGS</b>	Integrated electric-gas system		gasification at the time slot $t$
IES	Integrated energy system	$\eta_{elec,t}$	Reaction efficiency of PEM electrolysis at t
P2G	Power-to-gas	$\eta_{meth,t}$	Reaction efficiency of methanation at t
P2H	Power-to-hydrogen	$c_{ m H_2/CH_4}$	Concentration percentage of H <sub>2</sub> /CH <sub>4</sub>
P2M	Power-to-methane	$\pi_m$	The square of the pressure value at node <i>m</i>
PV	Photovoltaics	$\underline{\pi_m}, \overline{\pi_m}$	Threshold of the square of the pressure value of <i>m</i>
SOCP	Second-order cone programming	$\overline{p_m}, \overline{p_m}$	Threshold of pipeline pressure
WP	Wind power		
Paran	neters and constants	$\frac{S_m}{G}$ , $\overline{S_m}$	Threshold of natural gas source storage capacity
$\delta_{WP}$	Abandoning WP punishment parameter	$C_{\mathrm{CO}_2}$	Cost of CO <sub>2</sub> emissions
ρ	Hot spare coefficient	$C_i^f$	Coal consumption cost of thermal power unit <i>i</i>
LEL	Lower explosive limit of H <sub>2</sub> /CH <sub>4</sub>	$C_{m,t}^g$	Cost of the natural gas network
LFL	Lower flammability limit of H <sub>2</sub> /CH <sub>4</sub>	$C_{WP,t}$	Punishment cost of abandoning WP
UEL	Upper explosive limit of H <sub>2</sub> /CH <sub>4</sub>	$C_{Truck,t}$	Cost of truck transportation
UFL	Upper flammability limit of H <sub>2</sub> /CH <sub>4</sub>	$Cons_{\mathrm{H}_{2},t}$	Electricty consumption of producing H <sub>2</sub>
$C_{i,t}^{U/D}$	Start/Stop cost of unit <i>i</i> at time <i>t</i>	$E_{Coal,t}$	Profit from selling coal
$C_{mn}$	Weymouth constant	$f_{\mathrm{H}_{2},t}^{'}$	H <sub>2</sub> flow rate produced by P2G equipment for further
$H_i, J_i$	Single start / stop cost of unit i	2,	methanation at t
$R_d, R_u$	Unit down / up ramping speed	$f_{\mathrm{H}_2,t}$	H <sub>2</sub> flow rate produced by P2G equipment for hydrogen
	Minimum stop / start time		refueling station at t
	nd indices	$f_{mn}$	Natural gas flow from node <i>m</i> to node <i>n</i>
$\mathcal{N}_{\geq}$	Set of natural gas nodes, $\mathcal{N}_{\geq} = \{1, 2, \dots, m, \dots, N_g\}$	$M_{t}$	Weight of coal mined at the time slot t
$\mathcal{N}_{\mathcal{L}}$	Set of load nodes, $\mathcal{N}_{\mathcal{L}} = \{1, 2, \dots, i, \dots, N_L\}$	$p_m$	Pressure value of node <i>m</i>
$\mathcal{N}_{\mathcal{U}}$	Set of thermal units, $\mathcal{N}_{\mathcal{U}} = \{1, 2, \dots, i, \dots, N_U\}$	$P_{d,i,t}$	Load demand for electricity of node $j$ at time $t$
Varia	bles	$P_{i,\mathrm{max}}$	Maximum output value of unit i
$\alpha_t^{Truck}$	Transport consumption coefficient of hydrogen trucks	$P_{i,\mathrm{min}}$	Minimum output value of unit i
$f_{\mathrm{H}_{2},t}^{Coal}$	Flow rate produced by C2H at the time slot t	$P_{i,t}$	Output of thermal power unit $i$ at time $t$
$f_{\mathrm{H}_{2},t}^{Truck}$	Total hydrogen demand of heavy trucks at t	$P_{input/outj}$	$p_{out,i,t}$ Power flow input/output of node $i$ at $t$
$\alpha_t^{Coal}$	Efficiency of coal gasification at the time slot t	$P_{l,t}$	Power flow of line $l$ at time $t$
$lpha_{ ext{CH}_4 ext{elec},i}$	Power consumption parameter in process of electrolysis corresponding to CH <sub>4</sub>	$S_m$	Gas flow directly injected into the node $m$ from the source
$lpha_{ ext{CH}_4 ext{meth}}$	, Power consumption parameter in process of methanation corresponding to $\mathrm{CH}_4$	$u_{i,t}$	Start and stop status of unit <i>i</i> at time <i>t</i>

At present, some scholars are devoted to the research of hydrogen compressed natural gas (HCNG) equipment, and have achieved certain results in the study of the effect of hydrogen content percentage on integrated systems [4]. However, due to the characteristics of low density and high activity, blending hydrogen reduces the amount of energy delivered by the natural gas network under the same conditions. Hydrogen embrittlement may occur, which poses challenges to safety of the overall system. Due to the hazards of hydrogen embrittlement caused by the activity of hydrogen molecules, hydrogen buses in some cities is too high to make profits. some studies are devoted to solving the location of hydrogen embrittlement cracks and performing subsequent repair work of steel pipelines through precise positioning [7]. There-

fore, countries have established strict limits on hydrogen blending in natural gas networks (generally the volume of hydrogen is up to 6%) [8]. Then, the direct use of hydrogen converted by P2G technology in the CHP system involves multiple energy conversions, while each conversion is bound to bring about a large energy loss, so the gain is more than the loss. Also, High cost is the primary reason hindering largescale storage of hydrogen energy, mainly due to pressurized systems and containers. Moreover, the current input cost of

In a typical scenario of coal district, the conditions for the development of the hydrogen heavy trucks are unique: not only are hydrogen sources abundant, but also the application space of hydrogen heavy truck is broad. Different from the high hydrogen price in resource-deficient areas, the coal district has ample and cheap hydrogen, mainly from:

- More than 90% hydrogen is produced from fossil energy (e.g., coal, natural gas) or alcohols, which emits greenhouse gases[9];
- (2) Only 4% hydrogen is production obtained from renewable energy electrolysis, has more room for development[10] (Relatively stable WP is more suitable than PV with greater daily volatility).

Due to the huge demand for coal transportation in these areas, the number of locally registered heavy trucks is also very large, usually reaching tens of thousands. The reasons and significance of developing hydrogen heavy trucks are as follows:

- (1) Hydrogen heavy trucks can be directly developed, which are rigid demand, skipping low-profit fuel cell buses[11];
- (2) Fossil energy consumption and greenhouse gas emissions can be reduced by replacing diesel heavy trucks;
- (3) Compared with lithium power batteries, hydrogen heavy trucks are more suitable for heavy-duty and long-distance transportation, and have the advantages of longer cruising range, shorter charging time, and lighter weight;
- (4) Solar and wind energy can be effectively absorbed, and hydrogen can be used as a carrier of energy capture, avoiding the negative impact of electricity generated by renewable energy directly connected to the grid [12];
- (5) Electrolysis using renewable energy is usually the cleanest way, which can be considered as negative greenhouse gas production;
- (6) The current hydrogen produced by electrolysis in various countries only accounts for 4-6% of the total hydrogen production, which is still the main improvement direction and policy preference area.

#### 1.3. Contribution

In order to solve the above-mentioned challenges, models of hydrogen heavy trucks and P2G equipment are established and second-order cone programming (SOCP) are applied. The main contributions of this work are summarized below.

- (1) The closed industrial loop between coal mining, hydrogen production, truck transportation of coal, and integrated energy systems has been innovatively proposed.
- (2) P2G technology has been further expanded, by taking into account the detailed chemical reaction process of P2H and P2M. The proposed P2G technology adjusts electrolysis and methanation in real time to control the generation ratio of hydrogen and methane.
- (3) Reasonable use of hydrogen energy, as the fuel of hydrogen heavy trucks, is proposed, which avoids hydrogen embrittlement and reduces the storage cost.

(4) In the scenario of coal district, the models of hydrogen heavy truck, P2G equipment and IEGS are innovatively proposed. Incorporating heavy trucks into the unified dispatch of IEGS is conducive to making full use of hydrogen energy, reducing carbon emissions, and achieving clean and environmental protection.

The remaining parts of this paper are organized as follows. The scenario of coal district considering hydrogen heavy trucks and P2G equipment model are introduced in Section II. Section III describes the problem formulation and transformation. Case study is provided to prove the validity of the proposed model in Section IV. Section V draws the conclusion on this paper.

#### 2. Typical Scenario of Coal District

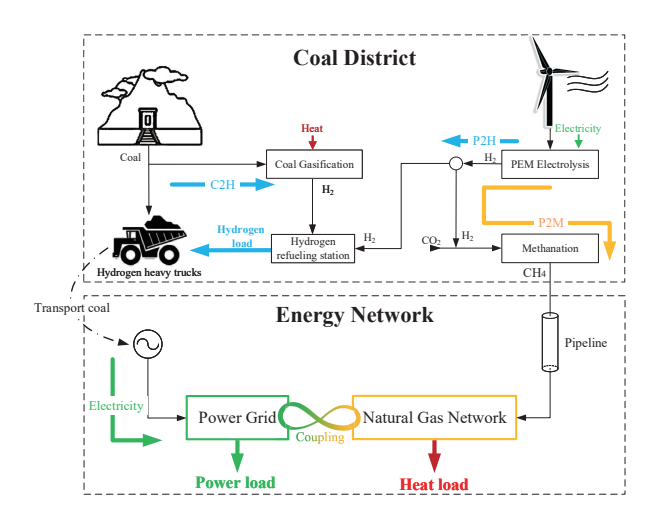


**Figure 1:** Scenario of coal district considering hydrogen heavy trucks and P2G equipment model of WP to H<sub>2</sub> and CH<sub>4</sub>.

As shown in Fig. 1, the closed industrial loop between coal mining, hydrogen production, truck transportation of coal, and integrated energy systems has been innovatively proposed.

### 2.1. Mining, processing and transportation

#### 2.1.1. Coal gasification

As summarized in section 1.2, more than 90% of hydrogen is produced by fossil energy, and the chemical reaction equation is as follows:

$$C + H_2O \xrightarrow{\triangle} CO + H_2 \Delta H = +131 \text{ kJ/mol}$$
 (1)

$$CO + H_2O \longrightarrow CO_2 + H_2 \Delta H = -41 \text{ kJ/mol}$$
 (2)

Due to the scenario of coal districts in this article, the process of producing hydrogen from fossil energy is only coal-to-hydrogen. Assuming that the weight of coal mined at the time slot t is  $M_t$  (ton), and  $\beta_t$  (%) is the ratio of mined coal used as the raw material for coal gasification, the amount of hydrogen produced by coal in this time slot is

$$f_{\mathrm{H}_2,t}^{Coal} = \alpha_t^{Coal}(\beta_t M_t) \tag{3}$$

 Table 1

 Comparison of heavy trucks with different power types.

	Hydrogen truck	Electric vehicle(EV)	Diesel oil truck
Filling time	10-15 min	Several hours	10-15 min
Recharge mileage	500-750 mile	100-300 mile	500-750 mile
	(Long-distance freight)	(Short-distance freight)	
Impact on the grid	Buffer	Relatively large	No impact
Energy sustainability	Promising	Depend on battery technology	Large price fluctuations, limited reserves
Emission	Zero	Zero	High

where  $\alpha_t^{Coal}$  represents the efficiency of coal gasification at the time slot t. This process is abbreviated as coal-to-hydrogen (C2H). Since the chemical reaction in (1) requires heat absorption, the reaction equipment involved in the process is also one of the heat loads.

#### 2.1.2. Hydrogen heavy trucks

Tab. 1 shows the comparison between hydrogen heavy trucks and electric vehicles and diesel trucks in many aspects. It can be predicted that in the future when hydrogen energy production technology continues to increase and costs continue to fall, hydrogen heavy trucks will become more competitive.

In the actual production process, the amount of coal mined is directly proportional to the required transport capacity of heavy trucks. In this article, the load capacity and required quantity of each heavy truck are no longer considered separately. But from a global perspective, the relationship between the hydrogen consumption of hydrogen heavy trucks and the amount of coal mining is as follows:

$$f_{\mathrm{H}_2,t}^{Truck} = \alpha_t^{Truck} (1 - \beta_t) M_t \tag{4}$$

where  $f_{\mathrm{H}_{2,t}}^{Truck}$  is the total hydrogen demand of heavy trucks at t and  $\alpha_t^{Truck}$  is the transport hydrogen consumption coefficient of trucks.  $(1-\beta_t)M_t$  represents the amount of coal that needs to be transported except for C2H.

#### 2.2. P2G equipment model

#### 2.2.1. Electrolysis & methanation technology

In the current field of industrial production of hydrogen, the main technology is proton exchange membrane (PEM) electrolysers. Electric conversion to hydrogen is achieved by electrolyzing water. The equation of the electrolyzed water reaction is shown in Eq. (5).

$$2 H_2 O \xrightarrow{\text{electrify}} 2 H_2 \uparrow + O_2 \uparrow \tag{5}$$

Methanation is the conversion of COx to methane  ${\rm CH_4}$  through hydrogenation. The reaction equations are shown in Eqs. (6) & (7) .

$$CO + 3 H_2 \longrightarrow CH_4 + H_2O \Delta H = -206 \text{ kJ/mol}$$
 (6)  
 $CO_2 + 4 H_2 \longrightarrow CH_4 + 2 H_2O \Delta H = -164 \text{ kJ/mol}$  (7)

#### 2.2.2. P2H and P2M model

P2H and P2M technology have their own characteristics:

- P2H has higher reaction efficiency than P2M;
- P2H technology conversion conditions is less difficult than P2M, and the required cost is low;
- Hydrogen cannot be injected into existing natural gas pipelines on a large scale, while methane can;
- Methane is safer in view of the flammability limits[13] and explosion limits[14];
- The production and combustion of hydrogen do not involve carbon emissions, and CO<sub>2</sub> is consumed during the production of methane;
- The calorific value of hydrogen is higher, which of methane is lower.
- a) Reaction efficiency constraints

$$\begin{cases} \eta_{elec,t} > \eta_{meth,t} \\ 57\% \le \eta_{elec} \le 73\% \\ 50\% \le \eta_{meth} \le 64\% \end{cases}$$
 (8)

where  $\eta_{elec,t}$  and  $\eta_{meth,t}$  are used to represent the reaction efficiency of the above two processes in the time slot t. Given two following assumptions:

- (1) In each time slot, the conversion efficiency of the electrolytic cell and methanation equipment  $\eta_{elec,t}$ ,  $\eta_{meth,t}$  remains unchanged, i.e., fixed value;
- (2) The chemical reaction process is a complete reaction and there is no reversible process.
- b) Conversion power consumption constraint

In the upper right corner of Fig. 1, the actual flow of the P2G equipment is drawn separately as Fig. 2, where each variable symbol (*e.g.*, flow rate and energy consumption parameters) is marked.

$$\begin{split} Cons_{\mathrm{H}_{2},t} &= \alpha_{\mathrm{H}_{2},t} f_{\mathrm{H}_{2},t} \\ Cons_{\mathrm{CH}_{4},t} &= \alpha_{\mathrm{CH}_{4} \mathrm{elec},t} f_{\mathrm{H}_{2},t}' + \alpha_{\mathrm{CH}_{4} \mathrm{meth},t} f_{\mathrm{CH}_{4},t} \\ &= 4\alpha_{\mathrm{CH}_{4} \mathrm{elec},t} f_{\mathrm{CH}_{4},t} + \alpha_{\mathrm{CH}_{4} \mathrm{meth},t} f_{\mathrm{CH}_{4},t} \\ \end{split} \tag{10}$$

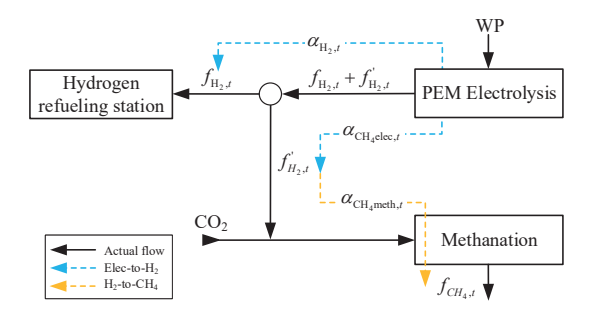


Figure 2: Schematic diagram of actual flow and variable symbols of P2G equipment.

where Cons<sub>H<sub>2</sub>,t</sub> represents the electric energy consumption used by the P2G equipment to produce H2 for hydrogen refueling station;  $f_{H_2,t}$  is the  $H_2$  flow rate for hydrogen refueling station at the time slot t;  $\alpha_{H_2,t}$  is the power consumption parameter corresponding to H<sub>2</sub> for hydrogen refueling station. Similarly,  $Cons_{CH_4,t}$  is the electric energy consumed to produce  $\mathrm{CH}_4; f'_{\mathrm{H}_2,t}$  is  $\mathrm{H}_2$  flow rate produced for further methanation;  $f_{CH_A,t}$  is the flow rate of  $CH_4$ ;  $\alpha_{CH_4 elec,t}$  represents the power consumption parameter in process of electrolysis corresponding to CH<sub>4</sub>, and  $\alpha_{\mathrm{CH_4meth},t}$  is that in process of methanation. In order to simplify the situation, only the chemical reaction described in (7) is considered here, that is, carbon dioxide and 4 times of the amount of the hydrogen produce methane under the action of high temperature and high pressure and a catalyst, i.e.,  $f'_{H_2,t} = 4f_{CH_4,t}$ . Therefore the second equality is established in Eq. (10).

#### c) Flammability& explosion limit constraint[13, 14]

The minimum concentration (%) of gas in the air under flammable conditions is defined as the Lower flammability limit (LFL), and the highest is the Upper flammability limit (UFL). Similarly, Explosion limits are expressed as lower explosive level (LEL) and Upper explosive limit (UEL), respectively.

$$\begin{cases} LFL_{H_2} \le c_{H_2,t} \le UFL_{H_2} \\ LEL_{H_2} \le c_{H_2,t} \le UEL_{H_2} \end{cases}$$
 (11)

$$\begin{cases} \mathrm{LFL}_{\mathrm{CH}_4} \leq c_{\mathrm{CH}_4,t} \leq \mathrm{UFL}_{\mathrm{CH}_4} \\ \mathrm{LEL}_{\mathrm{CH}_4} \leq c_{\mathrm{CH}_4,t} \leq \mathrm{UEL}_{\mathrm{CH}_4} \end{cases} \tag{12}$$

#### d) Calorific value constraint

The energy density of hydrogen is only about 25% of methane. When both release the same amount of energy, the volume of hydrogen is larger, and storage and transportation are more difficult. In this paper,  $q_{\rm H_2}=119.96$  MJ/kg,  $q_{\rm CH_4}=50.00$  MJ/kg.

#### 3. Problem Formulation

#### 3.1. Minimize long-term total costs

$$\min_{\mathbf{P},\mathbf{F},\mathbf{\Pi}} C_{total} = \sum_{i=1}^{N} \left( \sum_{i=1}^{T} C_i^f \left( P_{i,t} \right) + C_i^U + C_i^D \right) \tag{13}$$

$$+\sum_{m=1}^{N_g}\sum_{t=1}^{T}C_{m,t}^g+\sum_{i=1}^{T}C_{WP,t}+\sum_{i=1}^{T}C_{Truck,t}-\sum_{i=1}^{T}E_{Coal,t}$$

s.t.

(3), (4), (8) - (12)

$$\sum_{i=1}^{N_U} P_{i,t} = \sum_{i=1}^{N_L} P_{d,i,t}$$
 (14)

$$\sum P_{input,i,t} = \sum P_{output,i,t} \,\forall \text{power nodes}$$
 (15)

$$\sum_{i=1}^{N_U} \left( u_{i,t} P_{i,\text{max}} - P_{i,t} \right) \ge \rho \sum_{i=1}^{N_L} P_{d,i,t}$$
 (16)

$$u_{i,t} = \begin{cases} 0, \text{stop} \\ 1, \text{start} \end{cases}$$
 (17)

$$u_{i,t}P_{i,\min} \le P_i \le u_{i,t}P_{i,\max} \tag{18}$$

$$-R_{d} \le P_{i,t} - P_{i,t-1} \le R_{u} \tag{19}$$

 $\sum_{k=t}^{t+TS-1} (1 - u_{i,t}) \ge TS(u_{i,t-1} - u_{i,t})$  (20)

$$\sum_{k=t}^{t+\text{TO}-1} u_{i,k} \ge \text{TO}\left(u_{i,t} - u_{i,t-1}\right)$$
 (21)

$$C_{i,t}^{U} \ge \max\{H_i\left(u_{i,t} - u_{i,t-1}\right), 0\}$$
 (22)

$$C_{i,t}^{D} \ge \max\{J_i(u_{i,t-1} - u_{i,t}), 0\}$$
 (23)

$$P_{l,\min} \le P_{l,t} \le P_{l,\max} \tag{24}$$

$$\sum_{n|(m,n)\in A} f_{mn} = \sum_{n|(n,m)\in A} f_{nm} + s_m \quad \forall m \in \mathcal{N}_g \quad (25)$$

$$\operatorname{sign}(f_{mn}) f_{mn}^{2} \leq C_{mn}^{2} (p_{m}^{2} - p_{n}^{2}) \quad \forall m, n \in \mathcal{N}_{g}$$
 (26)

$$\operatorname{sign}(f_{mn}) = \begin{cases} 1, \text{flow direction is positive} \\ -1, \text{otherwise} \end{cases}$$
 (27)

$$\underline{s_m} \le s_m \le \overline{s_m} \quad \forall m \in \mathcal{N}_g \tag{28}$$

$$\underline{p_m} \le p_m \le \overline{p_m} \quad \forall m \in \mathcal{N}_g \tag{29}$$

where the coal consumption cost function  $C_i^f$  of thermal power unit i can be expressed by the following quadratic equation:

$$C_{i}^{f}(P_{i,t}) = a_{i}P_{i,t}^{2} + b_{i}P_{i,t} + c_{i}$$
(30)

where  $C_i^U$  represents the start-up cost of unit i,  $C_i^D$  represents the shutdown cost of unit i,  $C_{m,t}^g$  represents the cost of the natural gas network. For simplification, it is assumed that the punishment cost of abandoning WP  $(C_{WP,t})$  is linearly positively related to the amount of electricity abandoning.  $C_{Truck,t}$  indicates the cost of truck transportation, which is

positively related to the load capacity of the truck, when the load does not exceed the load capacity of the truck.  $E_{Coal,t}$  indicates the profit from selling coal, which is proportional to the weight of coal transportation. Constraints Eqs. (14)-(24) are related to the power system, including power balance constraint, hot spare constraint, unit output constraint, unit ramp constraint, unit start and stop time constraint, start & stop cost constraint and line power flow safety constraint. And Eqs. (25)-(29) are related to the Natural gas system system, including flow balance constraint, Weymouth equations constraint[15], source quantity constraint and pressure range constraint.

#### 3.2. Problem transformation based on SOCP

In the unified power flow modeling and solving, the SOCP-based power flow model has been used in network planning [1] with binary decision variables, and the problems generated are all modeled as mixed integer SOCP (MISOCP) [16].

In order to eliminate the non-linearity caused by pressure variables, make the following variable substitutions  $\pi_m = p_m^2$ . Thus, the constraint (29) can be rewritten as the following formula

$$\pi_m \le \pi_m \le \overline{\pi_m} \quad \forall m \in \mathcal{N}g$$
 (31)

The non-convexity of the steady-state flow model is derived from Eq. (26), where the absolute value sign  $(f_{mn})$  is non-smooth and non-differentiable. To solve this problem, a pair of binary variables  $f_{mn}^+$  and  $f_{mn}^-$  are introduced to represent the forward and backward flow directions of the pipe m-n, respectively. Therefore, Eq.26 is equivalently replaced with

$$\left(\frac{F_{mn}}{C_{mn}}\right)^{2} = \left(f_{mn}^{+} - f_{mn}^{-}\right)\left(\pi_{m} - \pi_{n}\right) \forall m, n \in \mathcal{N}g$$
(32)

By using bilinear relaxation, the bilinear term on the right side of (32) can be replaced by (33)-(37) (Note that since  $f_{mn}^+$  and  $f_{mn}^-$  are binary variables, this relaxation is strict):

$$\left(\frac{F_{mn}}{C_{mn}}\right)^2 = \lambda_{mn} \quad \forall m, n \in \mathcal{N}g$$
 (33)

$$\lambda_{mn} \ge \pi_n - \pi_m + \left( f_{mn}^+ - f_{mn}^- + 1 \right) \left( \pi_m^l - \pi_n^u \right)$$
 (34)

$$\lambda_{mn} \geq \pi_n - \pi_m + \left(f_{mn}^+ - f_{mn}^- - 1\right) \left(\pi_m^u - \pi_n^l\right) \quad (35)$$

$$\lambda_{mn} \geq \pi_n - \pi_m + \left(f_{mn}^+ - f_{mn}^- + 1\right) \left(\pi_m^u - \pi_n^l\right) \quad (36)$$

$$\lambda_{mn} \ge \pi_m - \pi_n + (f_{mn}^+ - f_{mn}^- - 1) (\pi_m^l - \pi_n^u)$$
 (37)

Eq. (33) can be relaxed according to the cone format shown in (38), where the standard SOC formula of (38) is expressed as

$$(F_{mn}/C_{mn})^2 \le \lambda_{mn} \quad \forall m, n \in \mathcal{N}g$$
 (38)

$$\left\| \begin{array}{c} 2F_{mn}/C_{mn} \\ \lambda_{mn} - 1 \end{array} \right\|_{2} \le \lambda_{mn} + 1 \tag{39}$$

#### 4. Case study

#### 4.1. Software and solving tools

In order to verify the effectiveness of the method in this paper, the above optimization program was developed using MATLAB-YALMIP platform, and the CPLEX algorithm package was used to solve the nonlinear mixed integer programming problem. The hardware environment of the test system is Intel (R) Core (TM) i7-6500M CPU @ 2.50 GHz, 8 GB RAM, Win10 64 bit (operating system), Matlab R2019b (development environment), and the YALMIP version is R2020.

IBM CPLEX ILOG is a high-performance mathematical programming solver for linear programming, mixed integer programming. The unit commitment problem is essentially a mixed integer programming (MIP) problem, which can be solved by MATLAB/CPLEX.

#### 4.2. Initial data

As shown in Fig. 3, the data of IEEE 30-node power system is utilized, and the rest of the data is shown in Tab. 2. The IEEE 30-node test case represents a part of the American power system (located in the Midwest of the United States). The original IEEE 30-node scenario considers the processing conditions of 6 thermal power units. Here, Unit 6 connected to node 8 is changed to WP equipment.

The natural gas network data adopts Belgium 24-node network data [15]. According to the internationally accepted natural gas sales rules, natural gas is priced according to its calorific value. The commonly used unit is Million Britain Thermal Unit (MBTU), while China's natural gas transaction is based on volume as a reference and the unit is cubic meter ( $m^3$ ). It is known that 1 MBTU  $\approx 28.3~m^3$ , and the unit conversion can be obtained: 1 \$/MBTU  $\approx 0.035~$ \$/  $m^3$ .

The maximum value of daily output power of the WP unit is set as 15,000 kW. The fluctuation data of WP output in each period is based on the project data of the University of Queensland in Australia. Now the unit output is increased by 30 times. Set the abandoning WP punishment parameter  $\delta_{WP} = 0.08$  \$/kWh.

#### 4.3. Simulation result

#### 4.3.1. Typical daily operating cost

The WP output data from February 27, 2019 to February 27, 2020 are selected, and the operation results in the proposed IEGS are shown in Fig. 4. The WP output at the same time basically conforms to winter>annual>summer, in which winter is selected from December to February of the following year, and summer is selected from June to August. Combined with the weather data measured by the wind project, WP output is influenced by natural factors such as temperature, wind speed and so on.

On the basis of ensuring the stable operation of WP output, in order to show the characteristics of energy-saving, clean, and fast absorption of P2G equipment, the comparison results obtained are shown in Tab. 3. Due to the independent operation of the power system and the natural gas system, and the direct connection of WP units to the grid, the electricity-gas system lacking a coupling and mutual aid

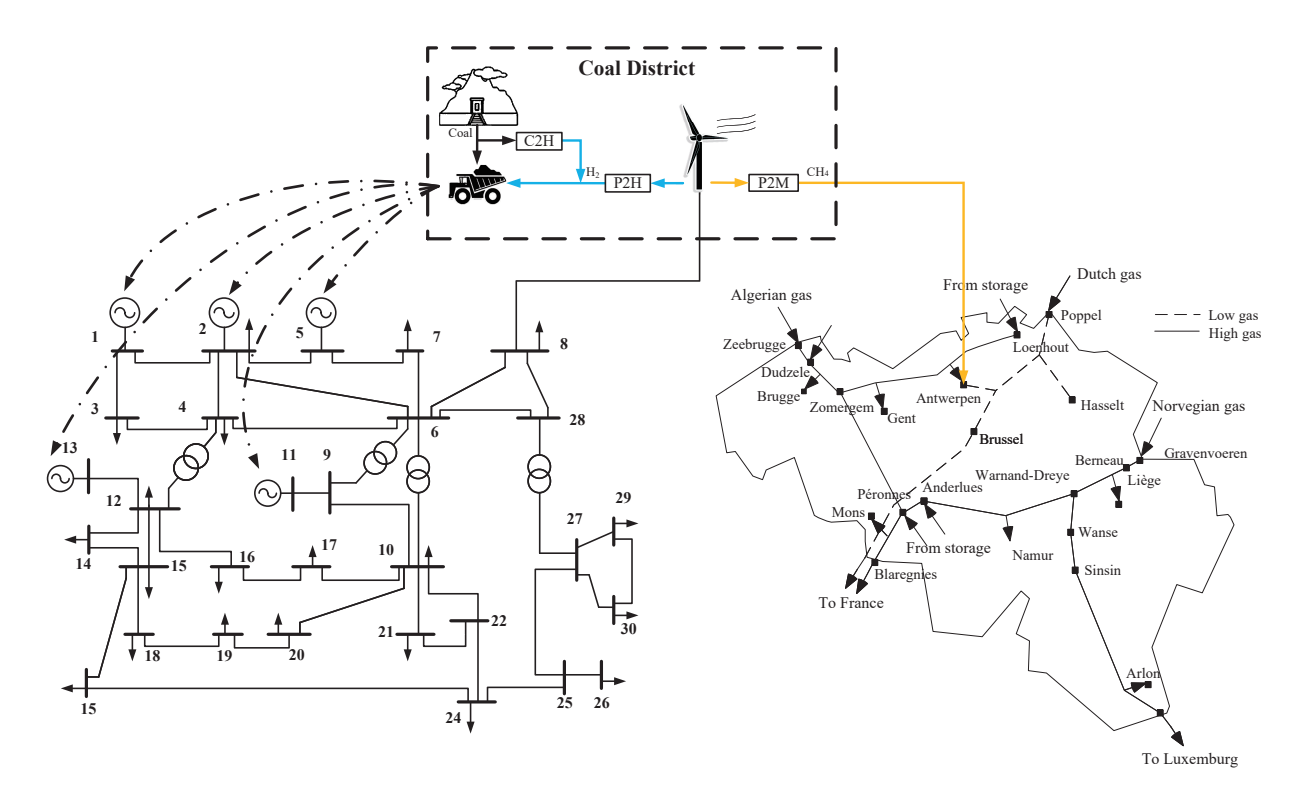


Figure 3: IEGS case study diagram.

Table 2
Initial data of thermal power units.

Unit	Node	P <sub>max</sub> (p.u.)	P <sub>min</sub> (p.u.)	a (ton/(p.u.) <sup>2</sup> )	b (ton/(p.u.))	c (ton)	$R_u/R_d$ (p.u./h)	TS/TD (h)	H (\$/time)	J (\$/time)
1	1	1.57	0.50	01524	38.5390	786.798	0.37	2	3937	19686
2	2	1.00	0.25	0.1058	46.1591	945.633	0.30	2	25000	12500
3	5	0.60	0.15	0.0280	40.3965	1049.998	0.15	2	15000	7500
4	8	0.80	0.20	0.0354	38.3055	1243.531	0.20	2	20000	10000
5	11	0.40	0.10	0.0211	36.327	1658.570	0.15	2	10000	5000

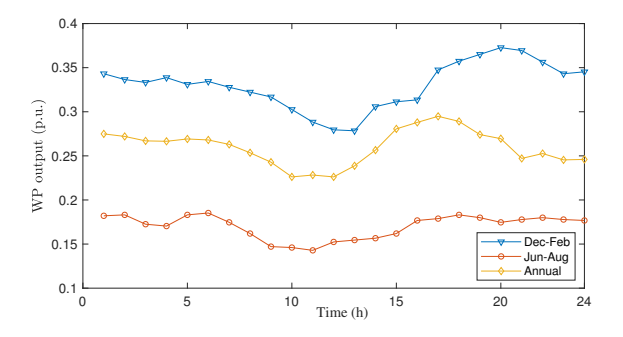


Figure 4: Typical daily WP output line chart.

relationship cannot absorb unstable and intermittent WP in a timely manner. In particular, the cost of abandoning WP is penalized, leading to higher operating costs for the IEGS without P2G equipment. If the ecological benefits brought by the consumption of carbon dioxide gas by P2G equipment

**Table 3**Comparison of total operating costs with or without P2G.

Total operating costs (\$/day)	with P2G	without P2G	
	$9.50763 \times 10^6$	$10.30285 \times 10^6$	

are taken into consideration, the advantages of P2G equipment are more prominent.

#### 4.3.2. Low-carban

Select 14:00 data to draw Fig. 5, which is based on the annual WP output. It can be seen that among the initial energy sources, electricity and natural gas come from the power system and the natural gas system respectively, and renewable energy accounts for a considerable proportion. Through transitional energy conversion, the initial energy can be transformed into hydrogen (supplied to hydrogen

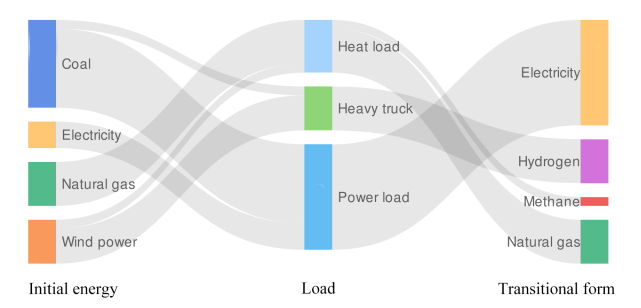


**Figure 5:** The energy conversion Sankey diagram of the proposed IEGS.

**Table 4**Comparison of total operating costs considering carbon emissions trading.

Total operating costs (\$/day)	China	European Union		
Hydrogen truck	$9.47361 \times 10^6$	$9.34901 \times 10^6$		
Electric vehicle	$9.56402 \times 10^6$	$9.58834 \times 10^6$		
Diesel oil truck	$9.91750 \times 10^6$	$10.20187 \times 10^6$		

heavy trucks), methane (can be directly injected into natural gas pipelines) and electricity (from power plants close to energy-consuming terminals).

In order to alleviate the greater environmental pressure and implement carbon neutral initiatives, carbon emissions trading is considered in this section[17, 18]. According to the Status Report 2019 of International Carbon Action Partnership (ICAP), emissions trading systems of most countries in the world currently are in force, scheduled or under consideration. This article uses the carbon emissions trading of China and the European Union as a measurement standard, and calculates the operating costs of the three heavy trucks mentioned in subsection 2.1.2.

According to the results of carbon emissions trading in 2020, prices in China are about 30-40 \(\frac{1}{2}\)/tCO<sub>2</sub>, but that in the EU has exceeded 30 €/tCO<sub>2</sub>. Taking into account carbon emissions trading, the revised total cost is  $(C_{total} - C_{CO_2})$ , where  $C_{\text{CO}_2}$  indicates the cost of  $\text{CO}_2$  emissions and proportional to the amount of CO<sub>2</sub> emissions. Tab. 4 shows that diesel oil trucks or LNG trucks will be levied high carbon emission fees, which will continue to increase as carbon neutrality advances. The current price of hydrogen heavy trucks is basically similar to that of electric vehicles, because in the proposed scenario, the methanation process can absorb a part of CO<sub>2</sub>. Therefore, hydrogen heavy trucks can not only achieve zero emissions on the basis of electric vehicles, but also absorb greenhouse gases, which are converted into profits here. With the continuous breakthrough of hydrogen energy technology and the inclination of government policies, the price of hydrogen energy will gradually drop and the scale of production will gradually expand. Further, hydrogen heavy trucks will have a broader prospect.

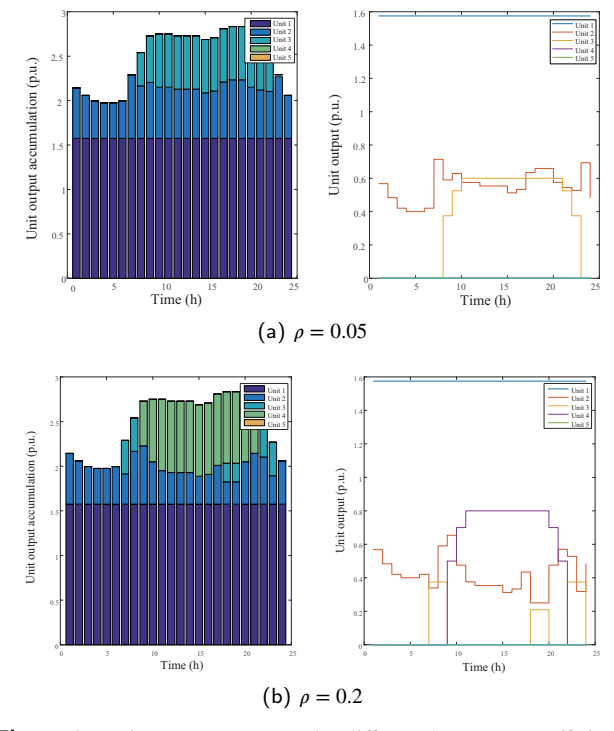


Figure 6: Unit output curves under different hot spare coefficient.

#### 4.3.3. Unit output curve

When the hot spare coefficient  $\rho$  is 0.05, the cumulative output ladder diagram of the unit is shown on the left side of Fig. 6-(a), which is basically in line with the distribution characteristics of power consumption peaks and valleys in reality, that is, there is a peak power consumption around noon during the day. In order to characterize the output status of each unit, draw the ladder diagram on the right side of Fig.6-(a). Each curve is basically stable, and there are no several start and stop conditions within a short period of time, which plays a good role in the overall stability of the system.

Similarly, when the unit hot spare coefficient is 0.2, Fig. 6-(b) are available. The cumulative output ladder diagram of the unit is shown on the left side of Fig. 6-(b). The ladder diagram on the right side of Fig. 6-(b) shows the output status of each unit and the curves are basically stable. However, some problems can be found in comparison with  $\rho$ =0.05. The right side of Fig. 6-(b) shows that the output of one unit has a short start and stop near 19:00, which is caused by the higher hot spare. Under the premise that a certain unit operating life and system stability are lost, the system's ability to respond to emergencies can be greatly improved.

## 4.3.4. Sensitivity analysis of abandoning WP punishment parameters

In this section, adjust the abandoning WP punishment parameters appropriately, set to four values of 0.01, 0.05, 0.08, and 0.12 respectively. The operation results of IEGS are shown in Tab. 3. When the abandonment punishment parameter is too small, the operating cost is higher, second only to the operating cost under the condition of no P2G

**Table 5**Comparison of total operating costs with different abandoning PV punishment parameters.

Abandoning PV punishment parameters (\$/kWh)	Total operating costs (\$/day )
0.01	$10.02773 \times 10^6$
0.05	$9.54392 \times 10^6$
0.08	$9.50763 \times 10^6$
0.12	$9.84057 \times 10^6$

equipment, indicating that even if the punishment parameter is small, the amount of abandonment is large, which still leads to the system. The overall operating cost is high. With the increase of the abandonment punishment parameters, the operating cost of the system has been significantly reduced, which proves that considering the abandonment punishment cost in the optimization objective can make the system fully absorb PV power. However, if the punishment parameters for abandoning solar energy continue to increase, the operating cost of the system will increase. This is because a small amount of unconsumed PV will be multiplied by a larger punishment coefficient, which will cause a certain punishment cost.

Further, as shown in the dotted line in Fig. 7, it can be estimated that although there is a nonlinear relationship between the abandoning WP punishment parameter and the operating cost, there should be a minimum value as shown in Fig. 7. When the abandonment punishment parameter takes this value, the total operating cost of the system is the smallest, and the specific value needs to be further explored. Moreover, when the abandoning WP punishment parameter is less than the optimal value, the curve drops faster, and the difference between the values of the abandoning WP punishment parameter is not very large, but a large amount of abandonment energy multiplied by it will cause a larger punishment cost. Correspondingly, when the abandoning WP punishment parameter is greater than the optimal value, even if the abandoning WP punishment parameter becomes significantly larger, the cost curve rises slowly because the amount of abandonment remains at a small amount.

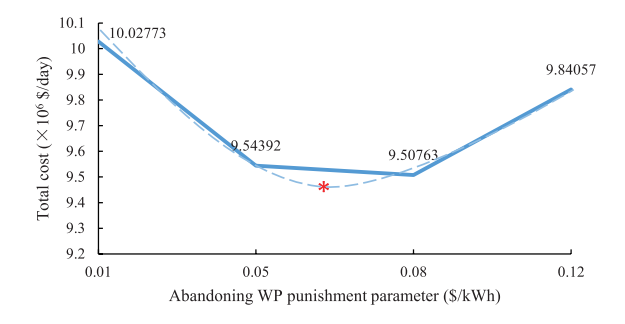


**Figure 7:** Curve line chart of the influence of  $\delta_{WP}$  on  $C_{total}$ 

#### 5. Conclusion

In view of the gradual transformation of the energy structure and the continuous development of the Energy Internet, IESs are important research direction. This paper draws the following conclusions:

- (1) Typical daily operating cost is significantly reduced by 7.7%, by introducing the P2G model which converts seasonally volatile wind energy into hydrogen and methane.
- (2) Hydrogen heavy trucks have certain advantages in the proposed coal districts scenario, *e.g.*, zero emissions and indirect consumption of renewable energy. Especially after the introduction of carbon emissions trading, the cost advantage is more prominent, compared with electric vehicles and diesel oil trucks.
- (3) The proposed P2G equipment and C2H technology improve the ability to absorb WP, enhance the reliability of the system, and solve the problem of volatility. More importantly, the mechanism in the article circumvents the potential risks caused by hydrogen mixing in natural gas pipelines, the cost of which cannot be measured.
- (4) The abandoning WP punishment parameter is considered in this article, and the optimal parameter is formulated according to the actual situation, which plays a certain guiding role for the future energy market leverage.

#### Acknowledgments

This work was supported in part by the Natural Science Foundation of Jiangsu Province (BK20181283).

#### **CRediT** authorship contribution statement

Junjie Yin: Conceptualization of this study, Methodology, Software, Formal analysis, Investigation, Data Curation, Writing - Original Draft, Visualization. Jianhua Wang: Validation, Resources, Writing - Review & Editing, Supervision, Project administration. Jun You: Writing - Review & Editing, Visualization, Supervision, Project administration.

#### References

- Y. Zhang, P. E. Campana, Y. Yang, B. Stridh, A. Lundblad, J. Yan, Energy flexibility from the consumer: Integrating local electricity and heat supplies in a building, Applied Energy 223 (2018) 430–442.
- [2] C. Sheng, Z. Wei, G. Sun, et al., Steady state and transient simulation for electricity-gas integrated energy systems by using convex optimisation, IET Generation, Transmission & Distribution 12 (2018) 2199–2206.
- [3] G. Gahleitner, Hydrogen from renewable electricity: An international review of power-to-gas pilot plants for stationary applications, International Journal of Hydrogen Energy 38 (2013) 2039–2061.
- [4] S. Zhou, K. Sun, Z. Wu, et al., Optimized operation method of small and medium-sized integrated energy system for P2G equipment under strong uncertainty, Energy 199 (2020) 117269.
- [5] L. Ni, W. Liu, F. Wen, Y. Xue, Z. Dong, Y. Zheng, R. Zhang, Optimal operation of electricity, natural gas and heat systems considering integrated demand responses and diversified storage devices, Journal of Modern Power Systems and Clean Energy 6 (2018) 423–437.

- [6] Y. Qiu, S. Zhou, J. Wang, J. Chou, Y. Fang, G. Pan, W. Gu, Feasibility analysis of utilising underground hydrogen storage facilities in integrated energy system: Case studies in china, Applied Energy 269 (2020) 115140.
- [7] Y. Chen, H. Lu, J. Liang, A. Rosenthal, H. Liu, G. Sneddon, I. Mc-Carroll, Z. Zhao, W. Li, A. Guo, et al., Observation of hydrogen trapping at dislocations, grain boundaries, and precipitates, Science 367 (2020) 171–175.
- [8] IEA, Limits on hydrogen blending in natural gas networks, 2018, Technical Report, IEA, Paris, 2020. https://www.iea.org/data-and-statistics/charts/ limits-on-hydrogen-blending-in-natural-gas-networks-2018.
- [9] K. Kunstle, C. Koch, K. Reiter, Coal gasification apparatus, 1978. United States Patent No. 4095959, https://www.freepatentsonline.com/4095959.html.
- [10] G. Pan, W. Gu, H. Qiu, Y. Lu, S. Zhou, Z. Wu, Bi-level mixed-integer planning for electricity-hydrogen integrated energy system considering levelized cost of hydrogen, Applied Energy 270 (2020) 115176.
- [11] J. Rolink, C. Rehtanz, Large-scale modeling of grid-connected electric vehicles, IEEE Transactions on Power Delivery 28 (2013) 894–902.
- [12] X. Wu, H. Li, X. Wang, W. Zhao, Cooperative operation for wind turbines and hydrogen fueling stations with on-site hydrogen production, IEEE Transactions on Sustainable Energy 11 (2020) 2775–2789.
- [13] ISO 10156:2017(en), Gas cylinders-Gases and gas mixtures-Determination of fire potential and oxidizing ability for the selection of cylinder valve outlets, Technical Report, ISO, 2017. https: //www.iso.org/obp/ui/#iso:std:iso:10156:ed-4:v1:en.
- [14] ISO/IEC 80079-20-1:2017, Explosive atmospheres Part 20-1: Material characteristics for gas and vapour classification Test methods and data, Technical Report, ISO/IEC, 2017. https://webstore.iec.ch/publication/26577.
- [15] C. Borraz, R. Bent, S. Backhaus, H. Hijazi, P. V. Hentenryck, Convex relaxations for gas expansion planning, INFORMS Journal on Computing 28 (2016) 645–656.
- [16] L. Badesa, F. Teng, G. Strbac, Pricing inertia and frequency response with diverse dynamics in a mixed-integer second-order cone programming formulation, Applied Energy 260 (2020) 114334.
- [17] K. Ricke, L. Drouet, K. Caldeira, M. Tavoni, Country-level social cost of carbon, Nature Climate Change 8 (2018) 895–900.
- [18] X. Zhang, A. Löschel, J. Lewis, D. Zhang, J. Yan, Emissions trading systems for global low carbon energy and economic transformation, Applied Energy 279 (2020) 115858.